

# **Detecting Weakened Highway and Railroad Bridge Substructures at Deck Level**

by

Chris Mullen  
Elizabeth Ervin

Department of Civil Engineering  
University of Mississippi  
106 Carrier Hall  
University, MS 38677-1848

NCITEC Project No. UM 2013-26

conducted for

NCITEC

May 2016

## DISCLAIMER

*The contents of this report reflect the views of the authors, who are responsible for the facts and the accuracy of the information presented herein. This document is disseminated under the sponsorship of the Department of Transportation University Transportation Centers Program, in the interest of information exchange. The U.S. Government assumes no liability for the contents or use thereof.*

## ABSTRACT

The ability to detect damage in substructures of highway and railway bridges using modal vibration techniques performed at the superstructure deck level is investigated as a means to improve nondestructive testing evaluation in cases where visual inspection is difficult or impossible. Methodology initiated in a 2012 NCITEC project is extended here first through a limited experimental study of lab scale models of substructure subsystems in a variety of configurations. Tests are conducted on a shake table to assess variations in frequency and temporal dynamic response characteristics for the different configurations, and frequencies are compared with those obtained by simplified finite element analysis of the subsystems. Detailed finite element analysis is then performed to characterize the dynamic characteristics of two full scale three-span highway bridges accessible to the project team. The two bridges have similar superstructures consisting of composite steel girder decks but lie in different geologic formations such that one was designed with a deep foundation system and the other with a shallow one. Fixed base models highlight the significant difference in fundamental frequencies for the two structural systems even when the different foundations are not considered. Soil-structure interaction models are developed to incorporate the soil and foundation elements and account for scour conditions that are the subject of a recently completed 2013 project. The deep foundation or flexible system is used to characterize the effect of soil-structure interaction and the influence of damage scenarios on the dynamic characteristics. Damage scenarios are considered that consist of material deterioration in the form of softening modeled as reductions of the elastic modulus in various substructure elements of one of two central piers. By virtue of the companion study, a damage scenario is also considered in which symmetric scour of a stream bed occurs between the two central piers. The material deterioration scenarios do not produce noticeable changes in the modal frequencies of the flexible system whereas the scour scenario produces changes in modes involving horizontal movement of the deck mass that are potentially significant enough to be detectable by measurements made at deck level.

## **ACKNOWLEDGMENTS**

The work was in large part made possible by a grant to the University of Mississippi from the US Department of Transportation through its University Transportation Center program and associated National Center for Intermodal Transportation and Economic Competitiveness.

Academic and additional financial support was provided by the Department of Civil Engineering at the University of Mississippi.

Co-PI, Dr. Elizabeth Ervin, Associate Professor in the Department of Civil Engineering, supervised all small scale lab testing performed at the Multi-Function Dynamics Laboratory which she established at the University of Mississippi. Graduate research assistants, Amir Irhayyim, Ai Nguyen, and Farhad Sedaghati assisted in the specimen preparation, measurements, data processing, and finite element modeling related to the lab testing.

Graduate research assistants, Trey Powell, Kim Tanner, Amir Irhayyim, and Farhad Sedaghati, in the Department of Civil Engineering at the University of Mississippi contributed to the detailed finite element modeling of the full-scale bridge case studies.

Bridge design drawings, soils data, and inspection reports were provided by the Bridge Division of the Mississippi Department of Transportation.

Geology related technical support and field survey information for the bridge case studies were provided by Charles Swann, R.P.G., of the Mississippi Mineral Resources Institute. Graduate Research Assistant, Kim Tanner, in the Department of Civil Engineering at the University of Mississippi coordinated data requests from the Mississippi Department of Transportation and contributed to the development of soils modeling data.

## TABLE OF CONTENTS

ABSTRACT.....	iii
ACKNOWLEDGMENTS .....	iv
TABLE OF CONTENTS.....	v
LIST OF TABLES.....	vii
LIST OF FIGURES .....	ix
INTRODUCTION .....	1
OBJECTIVE .....	7
SCOPE .....	9
METHODOLOGY .....	11
Laboratory Shake Table Experiments.....	11
Specimens .....	11
Loading and Instrumentation .....	15
Finite Element Modeling .....	18
Reference Cases.....	18
Damage Scenarios.....	24
DISCUSSION OF RESULTS.....	25
Laboratory Shake Table Experiments.....	25
Frequency Comparisons.....	25
Temporal Comparisons .....	30
Finite Element Simulations.....	34
Reference Case Modal Characteristics .....	34
Damage Scenario Modal Comparisons.....	41
CONCLUSIONS.....	43
RECOMMENDATIONS.....	44
ACRONYMS, ABBREVIATIONS, AND SYMBOLS .....	45
REFERENCES .....	47



## LIST OF TABLES

Table 1. Material properties.....	23
Table 2. Natural frequencies (Hz) resulting from tap and shake tests.....	26
Table 3. Natural frequencies and mode shapes resulting from finite element Model 1.....	28
Table 4. Natural frequencies and mode shapes resulting from finite element Model 3.....	29
Table 5. Comparison of experimental to modeled natural frequencies.....	30
Table 6. Maximum tri-axial accelerometer results for tested configurations.....	31
Table 7. Modal characteristics of fixed base reference models for two case studies.....	34
Table 8. Modal characteristics of reference models for flexible system.....	38
Table 9. Modal characteristics comparison of SSI models for flexible system.....	41





## LIST OF FIGURES

Figure 1. Locations of highway bridges in north Mississippi.....	1
Figure 2. Locations of railroad bridges on private lines in north Mississippi.....	2
Figure 3. US 178 bridge with deep foundation- embankment eroded by scour (B002).....	3
Figure 4. US 178 bridge with shallow foundation- footing exposed by scour (B005).....	3
Figure 5. Highway bridges along major corridor in northeast MS .....	4
Figure 6. I 55 bridge on very soft soil having batter piles on exterior of multi-pile bents.....	6
Figure 7. Railway bridge on deep foundation with piles exposed by scour.....	6
Figure 8. Assembly of Model 1.....	13
Figure 9a. As built Model 1.....	13
Figure 9b. As built Model 2.....	14
Figure 9c. As built Model 3.....	14
Figure 10. Tested configurations of Model 1.....	16
Figure 11. Xcitex ProAnalyst Interface for Model 1, 0.21 g, and 20.....	17
Figure 12. Flexible system reference model mesh.....	20
Figure 13. Flexible system part definition.....	21
Figure 14. Stiff system reference model mesh.....	22
Figure 15. Flexible system symmetric scour model mesh .....	24
Figure 16. Power spectra for Model 1 without soil .....	25
Figure 17. Failure of Model 1.....	33
Figure 18. Failure of Model 2.....	33
Figure 19. Fixed base modes for the flexible system .....	35

Figure 20. Fixed base modes for the stiff system .....	36
Figure 21. SSI modes for the flexible system involving horizontal deck movement.....	39
Figure 22. SSI modes for the flexible system involving vertical deck movement.....	40

## INTRODUCTION

Nearly 204 million daily crossings occur on 58,495 U.S. structurally deficient bridges in need of repair. So says the Association of Road and Transportation Builders Association based on data in the January 2016 release of the National Bridge Inventory (NBI 1). Of the 17,057 bridges in the database located in the state of Mississippi, 2184 bridges are defined as “structurally deficient”. This places Mississippi as 8<sup>th</sup> nationally for total number with that designation and 12<sup>th</sup> nationally as a percentage of the state’s inventory.

The large inventory of both highway and railroad bridges service corridors of importance to the economic competitiveness of the state linking neighboring major cities of Memphis, TN, Birmingham, AL, and New Orleans, LA. Figure 1 shows the major highway routes and bridge locations in the northern part of the state.

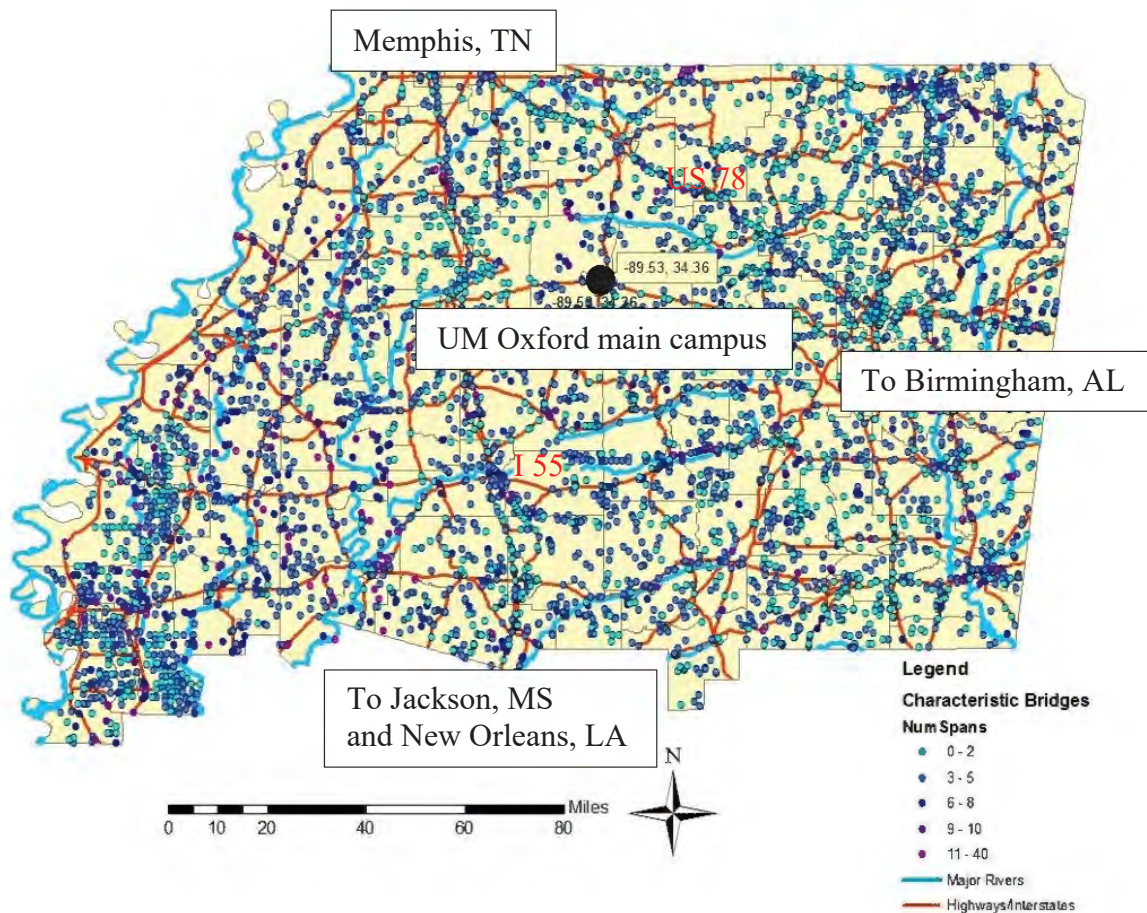


Figure 1. Locations of highway bridges in north Mississippi

\* Note: County bridges are shown but the routes on which they are located are not

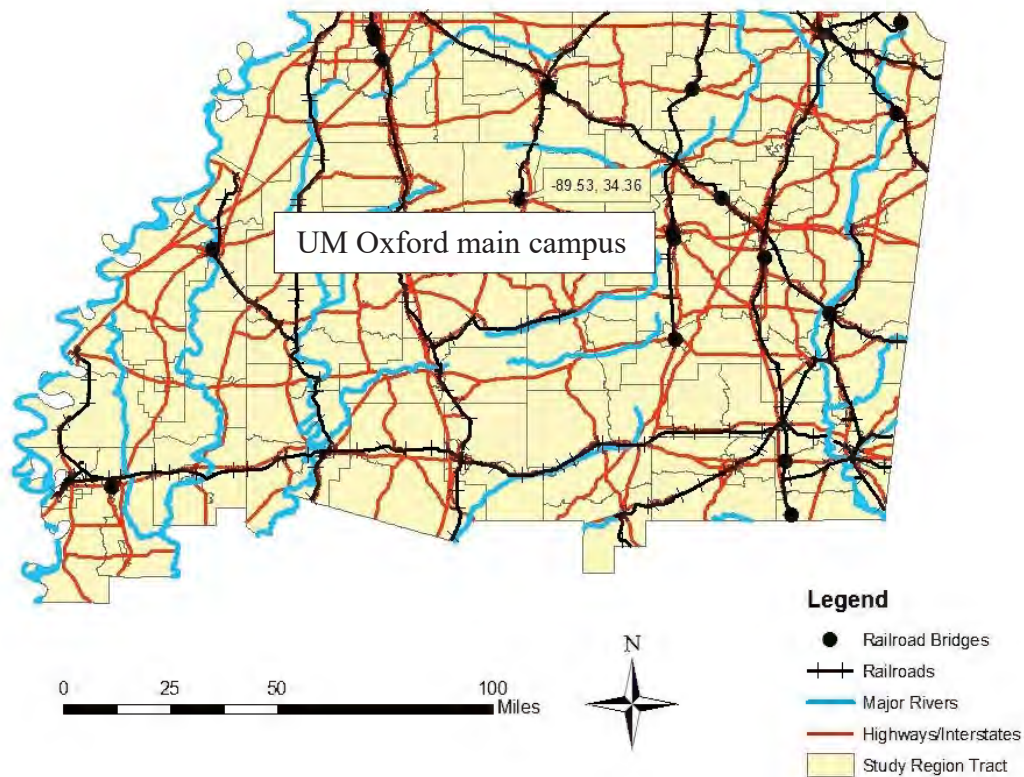


Figure 2. Locations of railroad bridges on private lines in north Mississippi

Located along these corridors are major manufacturing facilities that include two major automobile plants. It is thus of vital importance that the bridges servicing these corridors remain functional to ensure that the many communities and facilities that depend on them are not severely impacted.

The two bridges shown in Figures 3 and 4 have been selected as case studies for purposes of this study. The bridges were readily accessible to the project team and characterize a range of structure, foundation, and deterioration conditions that exist in the operational bridge inventory of the state. Both bridges are located on US 178 near one of the automobile plants located in the northeastern part of the state as shown in Figure 5. The route is part of the federal highway system, so the bridges are subject to federal inspection and reporting requirements which the state department of transportation oversees.





Figure 3. US 178 bridge with deep foundation- embankment eroded by scour (B002)



Figure 4. US 178 bridge with shallow foundation- footing exposed by scour (B005)

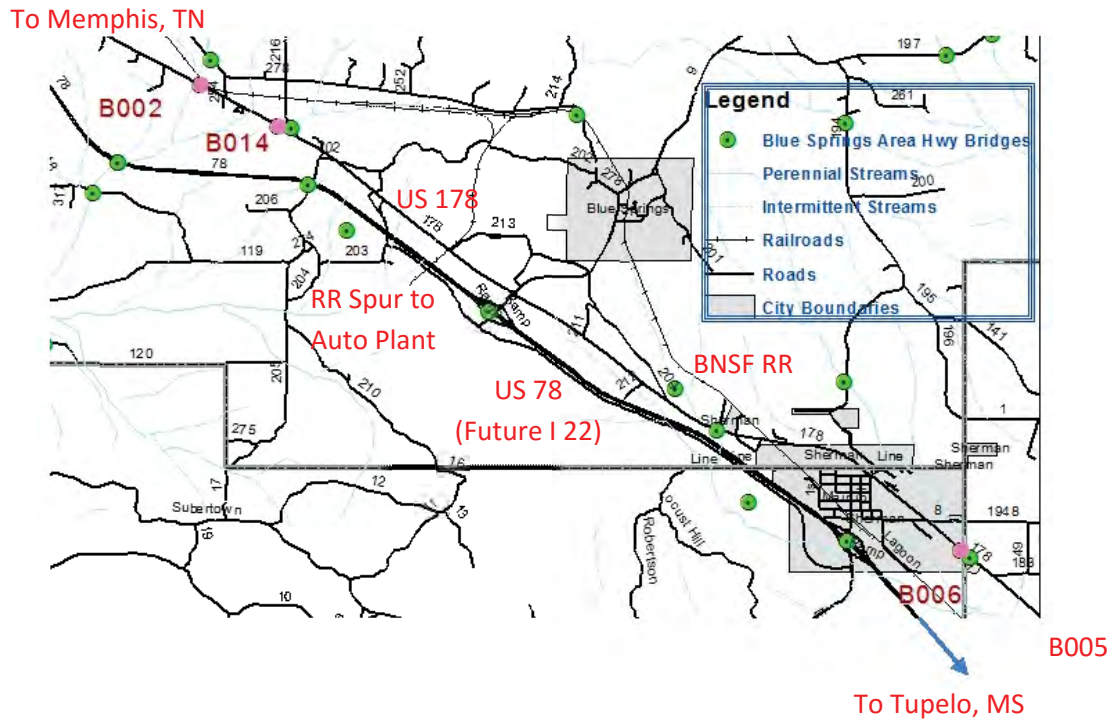


Figure 5. Highway bridges along major corridor in northeast MS

\* Note: Bridge numbers (B0XX) were assigned as part of a field condition survey

The study builds on the methods and findings of a 2012 NCITEC project (2) which explored the benefits of vibration based nondestructive testing (NDT) techniques applied to damage detection of highway and railway bridges. NDT techniques offer a cost-effective means of improving reliability of visual inspection procedures (3). As an example, the NBI database reports that inspection of the I 55 bridge shown in Figure 6 cost approximately \$2 M for each of three inspections performed in 1992, 2000, and 2010.

The 2012 study focused on vibrational response of the superstructure elements mostly in a lab scale setting in the presence of damage characterized by bearing stiffness properties. Here, the focus is on the influence on the deck vibration characteristics of the substructure elements of the complete in situ bridge system. Such elements include bearings, piers, abutments, and the foundation medium (soil or rock).

The substructure elements are difficult to access in visual inspections due to field conditions. The internal nature of some damage such as material deterioration makes visual inspection misleading or inconclusive. In the case of scour around submerged pier footings, visual inspection requires special mobilization including divers and underwater equipment (3).

Laboratory scale experiments on single pier and single span substructure subsystems are also performed to provide supporting information for simple cases to motivate a better understanding of the more complete soil-structure foundation systems. The configuration of the lab specimens has been motivated by the highway and railway bridges shown in Figures 6 and 7, respectively.

Detailed finite element (FE) models are then constructed for the complete full scale bridge systems representing the two case studies. Characteristic mode shapes and frequencies are identified by eigenvalue analysis of the FE system matrices. Such mode shapes provide a preliminary view of what is identifiable through modal extraction of field vibration measurement data. Damage here is limited to a variety of material deterioration cases as well as scour at the pier footing level. Scour conditions and their effects on the bridge system are studied in more detail in a companion 2013 NCITEC project (4).





Figure 6. I 55 bridge on very soft soil having batter piles on exterior of multi-pile bents



Figure 7. Railway bridge on deep foundation with piles exposed by scour



## OBJECTIVE

The present study builds on the methodology and findings of a 2012 NCITEC study (2). Whereas the earlier study focused on modal characteristics of the superstructure deck, the present one examines the modal characteristics of the substructure elements. The primary objective is to establish the feasibility of detecting damage in the substructure elements using deck level vibration measurements as were obtained in the 2012 study on a full scale operational highway bridge located on the University of Mississippi's main campus within the small town of Oxford, MS.

As was done in the 2012 study, both FE and experimental work is performed in the present one. Emphasis is given here to FE characterization in consideration of the extensive time, mobilization, and resources required for full scale field tests.

While the focus here is on complete bridge systems, insight is first sought through a limited set of tests on small scale laboratory specimens representing single spans in three common bridge pier configurations: railroad and highway cases with straight piles, and a highway case with batter piles.

Dynamic characteristics of each lab specimen case are assessed in both frequency and temporal domains using shake table excitation. Frequency analysis provides insight on modal vibration characteristics useful in tuning FE models, and temporal analysis provides insight on general response and stability patterns. Limited FE analysis is performed to visualize characteristic mode shapes of the specimens without soil.

Detailed FE models are then developed for the two case studies. Included are the full-scale superstructure (concrete deck and steel girders), substructure (concrete piers and abutments), foundations (concrete footing and wood piles), and supporting soil layers (sand/silt/clay or chalk). The presumption here is that, while the computational effort is significantly increased, it is the experience of the principal investigator that including all of the listed elements is essential to the successful identification of modal characteristics in a field environment.

Eigenvalue analysis is performed to obtain mode shapes and frequencies of the soil-structure interaction (SSI) models. An idealized reference model is first developed using information in design drawings and soils reports from the time of construction. The reference model is then modified to account for a variety of damage scenarios involving material deterioration in select substructure components or scour near select foundation elements.

Comparison of the modal characteristics of the damage and reference models provides the basis here for determining the sensitivity of field vibration measurements to a variety of substructure damage conditions. The results provide useful insight and guidance to future investigations involving application of field vibration based NDT and FE analysis using SSI models.

## SCOPE

The laboratory component of the project identifies three model configurations for shake table testing. Each model represents an idealized bridge pier or single span substructure subsystem covering a range of stiffness and response types. Tests are performed with and without influence of a limited amount of soil restraint. Comparison of frequency and temporal response is made of the measured data, and trends are examined across model types and dynamic loading characteristics. FE models of two of the model configurations enable mode shape visualization and comparison of frequency trends obtained using shake table test data.

The detailed FE modeling of full system behavior of two case studies first addresses a reference model corresponding to an idealized undamaged state. A set of three hypothetical damage scenarios are then examined involving material deterioration of substructure elements in one of the two central piers. To leverage modeling work for the scour project (4), a fourth scenario is defined representing severe scour in the stream bed between the two piers.

While no longer located on the primary highway route, the two case studies exemplify aging superstructures commonplace in the MS and US inventory. By virtue of their respective locations, they also permit the study of the effect on bridge system dynamic characteristics of two very different geologic formations, one relatively flexible and the other relatively stiff.

Both bridges used as case studies are accessible to the investigators enabling field surveys of current site conditions discussed in more detail in the scour study (4). The project team was also able to obtain design drawings, soil reports, and a limited set of inspection reports for these bridges from Bridge Division personnel at the Mississippi Department of Transportation located in Jackson, MS. The data enabled development of detailed reference models consistent with both design and construction practice as well as field observations.

The project team had hoped to use as a third case study an adjacent railroad bridge that shared the same geologic formation conditions as one of the highway bridges selected here. The railroad bridge exhibits severe scour that has exposed the piles of one of the piers. Unfortunately, attempts to gain the cooperation of the railroad owner's structural engineers were unsuccessful, and the project team was denied permission to access either the site or any engineering data that might assist in detailed FE modeling.

One of the geologic formations consists of a relatively flexible layer of soil that caused the bridge designer to select a deep foundation system consisting of concrete footings/pile caps supported on wood piling. The other formation consists of a thick chalk layer that caused the

bridge designer to select a shallow foundation system consisting of spread footings resting directly on the chalk layer. The bridge with the deep foundation system has experienced significant scour on one side due to channelization of the waterway beneath the bridge. The piled footings will likely become exposed during the service life of the bridge. The bridge with the shallow foundation has similarly experienced scour on one side that has already exposed the spread footings.

FE analysis consists of self-weight static analysis and subsequent eigenvalue extraction of detailed three-dimensional solid element based SSI models of the complete system. Adoption of the use of solid elements is motivated by the experience of the principal investigator during the 2012 study in which it was found that beam and shell elements were unable to sufficiently characterize, capture, and visualize localized behavior associated with the type of damage scenarios considered in this work.

# METHODOLOGY

## Laboratory Shake Table Experiments

### Specimens

The Multi-Function Dynamics Laboratory (5) staff built three separate models: a railroad bridge with minimum number of straight piles, a highway bridge with more straight piles, and a highway bridge with added battered piles. These configurations have increasing lateral stability, and this metric has been compared to FE models. Each configuration has been tested with two in-fill soils: sand and field soil. Thus, six configurations have been fabricated; one experienced premature failure, so five configurations were successfully tested.

Limiting model dimensions to 8.5x8.5x12 inches, acrylic containers were used to contain the models and soils. The graduations on the side of each container were placed in the longitudinal direction. The dimensions were also selected by scaling down the reference highway bridge approximately fifty times, except for column diameter due to material limitations.

Plaster of Paris was used as the structural material, and the manufacturer (DAP) promises a strength of 1,500 pounds per square inch (psi). The material behavior is similar to concrete, but steel rebar was not feasible. Cap, footing, and column pre-cast molds were constructed from kitchen gear; as in the field, the molds were oiled with a non-petroleum canola product for easy release. Plaster construction used clean water and then added dry plaster in a 2:1 ratio. Some variation was required due to humidity: less powder was allowed if more workability is required. The mixture was then gently stirred and poured into molds, and hand vibration and wire rodding was employed to prevent voids. Four pours were required, and cure time was at least two days.

Columns were formed by pouring plaster into acrylic tubing with an outer diameter of 1-3/16 inches. The total height of each straight column was 8.6 inches with a free height of 6.6 inches and 2 inches of embedment. Batter columns were just 1/10 of an inch longer, but its ends were constrained to be flat. Column ends were sealed with plastic wrap, and columns remained vertical throughout the curing process.

The caps were thick lumped masses, representing pier caps, deck, and roadway. A rectangular cap was selected to avoid any internal resonances. This also allowed more space (0.5 inches per side) for lateral motion than the longitudinal direction. The caps were

nominally 7.5x8.25x2 inches; the thickness prevented cracking and punch shear at columns. Two caps were be poured upside down in molds, and inserts generated one-inch deep holes for later straight or batter column assembly. The same aquarium tubing was cut for the inserts, and plastic wrap sealed the ends. The caps were open to air during curing.

To ensure proper fits at pile bottoms, a mat foundation of 1.5 inch thickness has been selected for each of the three footings. Each footing was epoxied to the container bottom to represent fixity as some soil layer. Footing size was maximized for stability. With straight columns, the footings were 8x8x1.5 inches; the thickness prevented cracking when attached to the container. The footing for the model with battered piles was slightly larger at 8x8.25x1.5 inches; the slanted holes required slightly more cover to prevent cracking. The footings were also poured upside down in molds, and inserts generated one-inch deep holes for later column assembly. Using a band saw bias cut, skewed inserts were employed for the battered piles. The footings were open to air during curing.

Resistant to any soil dampness, two-part epoxy was used to represent fixity during model construction. All columns were glued at the footings for stability. Cap connections for the rail configuration were also glued; however, the other configurations had moment release connections, which had waxed friction fit connections in the models.

This assembly process is shown in Figure 8. The three configurations without soil were tested first, and then each cap was removed to insert soil. Home Depot “play sand” was poured into the container, voids were removed, and testing was repeated. Lastly, field soil that was collected from a local Mississippi bridge site was prepared for installation. The soil was dried, broken into manageable pieces, then reconstituted with water for workability. The relatively homogeneous “muck” was then laid into the container, tamped in layers, and allowed to surface dry. The testing was repeated as before, except that a column was prematurely broken during the last field soil installation around the batter piles.

Final configurations are summarized in Figures 3a (Model 1), 3b (Model 2), and 3c (Model 3).



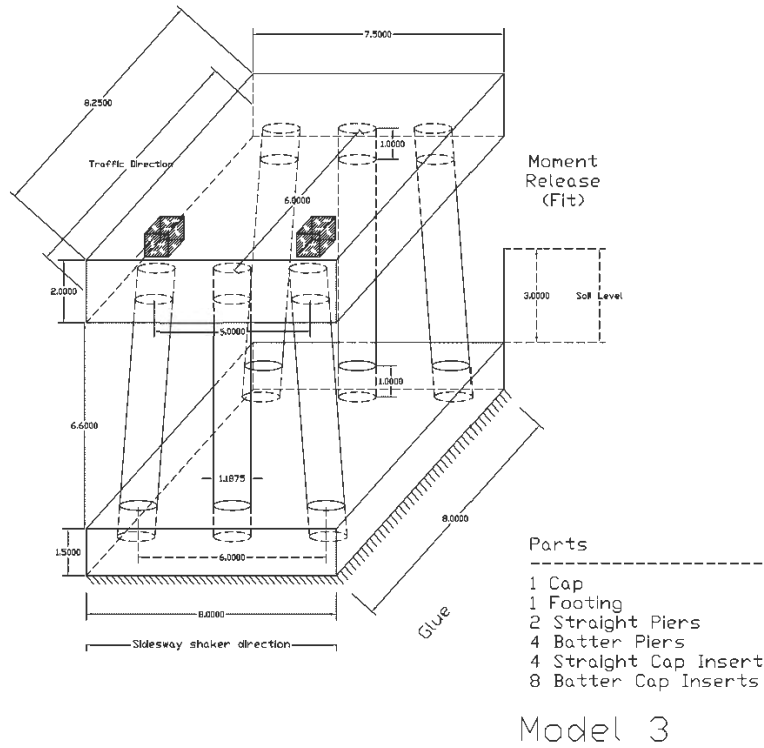


Figure 9b. As built Model 2

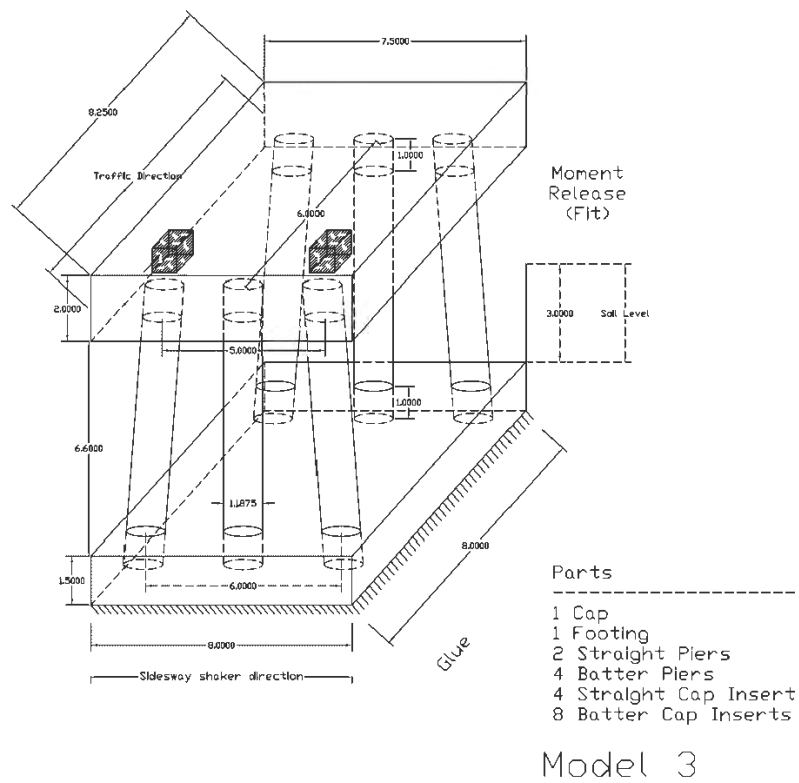


Figure 9c. As built Model 3



## Loading and Instrumentation

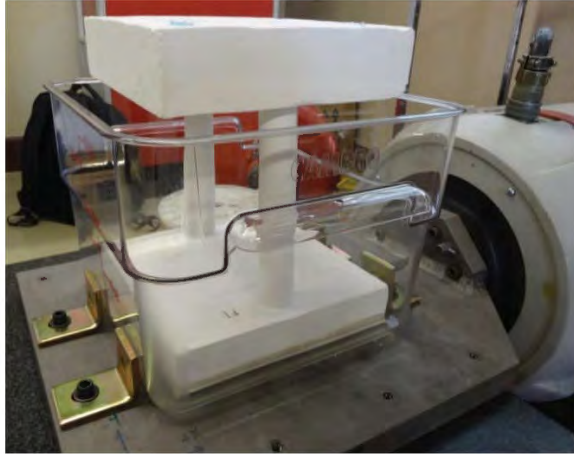
Before soil was added, tap tests were performed with an impact hammer (PCB Model 086D05) to examine frequency content of each structure. A shake table was then used to excite the model structures in a lateral, sidesway direction. As determined by the observed frequencies in the as-built configurations, sinusoidal excitation of 20 Hertz (Hz) was employed at the peak amplitudes of 0.10, 0.21, and 0.34 g.

The three tested configurations of Model 1 are shown in Figures 10a (no soil), 10b (sand), and 10c (field soil). Each photograph shows the 14x14 inch aluminum table platform with attached angle brackets securing the plastic vessels. The platform rides along an oil film on top of a leveled granite slab. The circular gray actuator is connected to a controller using the feedback of a table-mounted accelerometer. The red cabinet in the background is the 480V/3-phase amplifier.

Two instrumentation schemes were synchronously employed. To measure acceleration, two tri-axial seismic accelerometers (PCB Model 356B18) were placed over the two outer columns on one pier. The locations are noted in Figure 9 as hatched boxes; along with translations, these locations also indicate any rotation. The yellow boxes in Figures 10b and 10c are the in-place accelerometers connected by blue BNC cables to a National Instruments (NI) CompactDAQ data acquisition system. This is in turn connected via USB to a laptop running NI LabVIEW.

In addition, high-speed video was taken and analyzed for steady-state deflections. A Redlake Y4 (Kodak) with constellation lighting captured the cap motion at 1,000 to 4,000 frames per second at 1012x1012 pixel resolution. Cap deflections were visually tracked via the number stickers “1” and “2” shown in Figure 10c. Shown in Figure 11, ProAnalyst (Xcitex) was used to area tracking to measure deflections down to an amazing ten-thousandth of an inch. The threshold of 0.0065 inches per pixel causes the signal clipping in the green sinusoidal signal shown. Line tracking was also used in this software to extract rotations.

Other frequencies were run for educational purposes, and the high speed video was useful to show failure modes.



a. No soil



b. Sand



c. Field soil

Figure 10. Tested configurations of Model 1

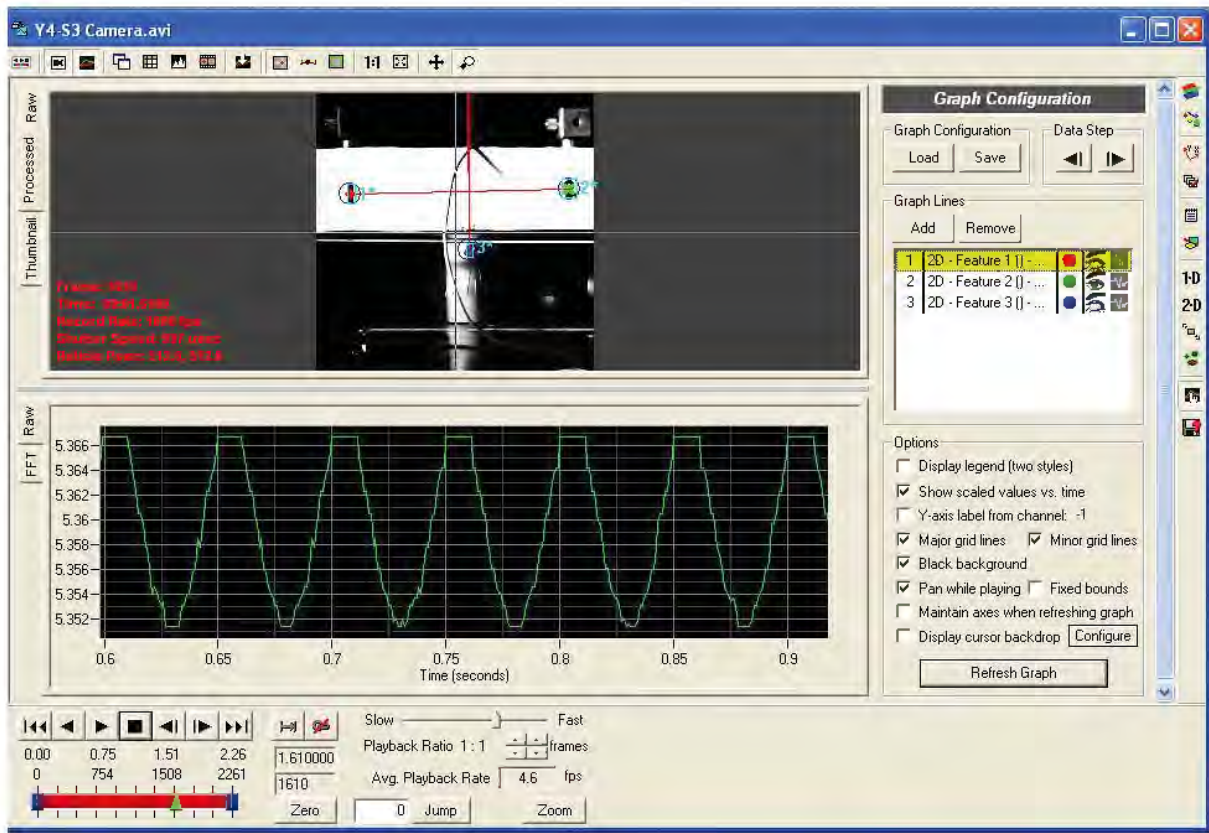


Figure 11. Xcitex ProAnalyst Interface for Model 1, 0.21 g, and 20

## Finite Element Modeling

### Reference Cases

The case studies selected for detailed FE modeling shown in Figures 3 and 4 each consist of three-span bridges having two reinforced concrete (RC) end abutments and two RC intermediate piers. Each bridge carries traffic across a stream whose alignment with respect to the highway and flow patterns have caused severe scour. Loss of soil is concentrated at the embankments and pier footings on the side where increased water velocity has been induced by the stream flow pattern.

The first case (Fig. 3) consists of two 30 ft. side spans and a 40 ft. center span. The superstructure is comprised of a RC deck slab poured compositely with four steel W-shape girders. Each girder rests on a steel bearing plate that is bolted into the top of a RC abutment or pier. There are no cross-bracing elements between girders.

The substructure abutments and piers are each comprised of two columns and a cap beam. The columns of the abutments are tapered, fully embedded in embankment soil, and supported on RC footings poured over a square pattern of four tapered wood piles. The columns of the piers are straight, partially embedded in soil, and supported by a similar piled footing configuration.

The soil consists of well-graded fill material placed above the natural deposits which consist of mainly stiff sand and silty sand layers.

The ABAQUS CAE modeling and analysis environment (6) has been selected for the study. The CAE software provides a powerful graphical user interface (GUI) that enables generation of virtually any geometry as well as automated mesh, load, boundary condition, and constraint generation. The GUI within CAE also enables interactive activation of the FE formulation and solution algorithms available in ABAQUS (7) as well as data checking, monitoring and post-processing of all results generated by the solution.

Three-dimensional (3D), 8-noded, continuum (solid, homogeneous), reduced-integration elements (C3D8R) have been selected to perform all modeling of components of the superstructure, substructure, and soil systems. These elements require only the nodal coordinates, the Young's modulus of elasticity, and the mass density to fully construct the element mass and stiffness matrices.

Figure 12 shows the fully meshed model geometry at subsystem and system levels for the first case study (Fig. 3). SSI has been enabled through an Embedded Region Interaction in

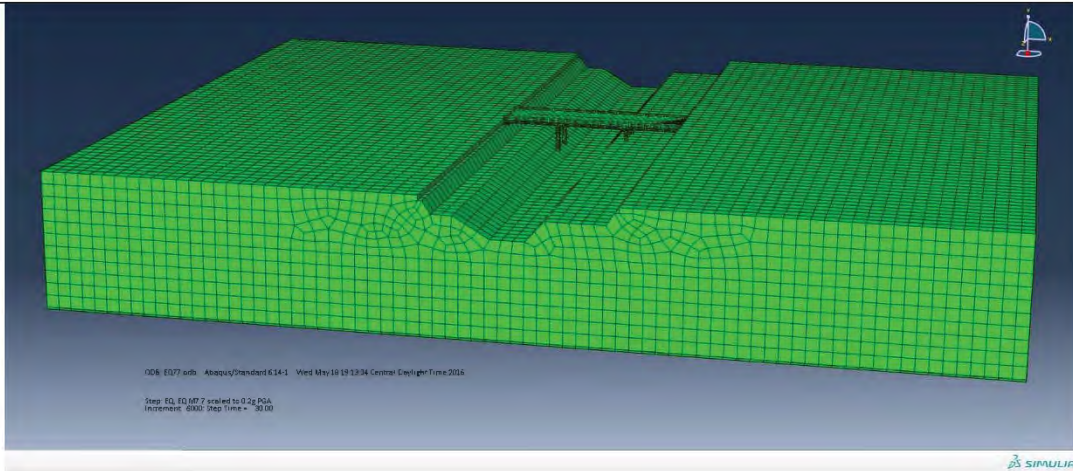
which the soil elements serve as the Host region. Piles are likewise embedded in the host footing regions. Reinforcing steel could in principle be embedded in the host concrete regions, but the contribution of the steel has been neglected in this study which is more concerned with relative effects on system dynamic characteristics induced by damage. In an FE model comparison with actual field investigation, the steel may need to be included to obtain reliable results.

All locations of contact have been treated as a Tie Constraint between the surfaces in contact. Such a constraint assumes full transfer of load. Slip is not allowed in this approach. Instances of contact surfaces arise in the bridge models at, for example, the interface between concrete deck slab and top flange of steel girders, the bottom flange of steel girders and top of bearing plate, and top of bearing plate and top of concrete abutment/pier cap beam.

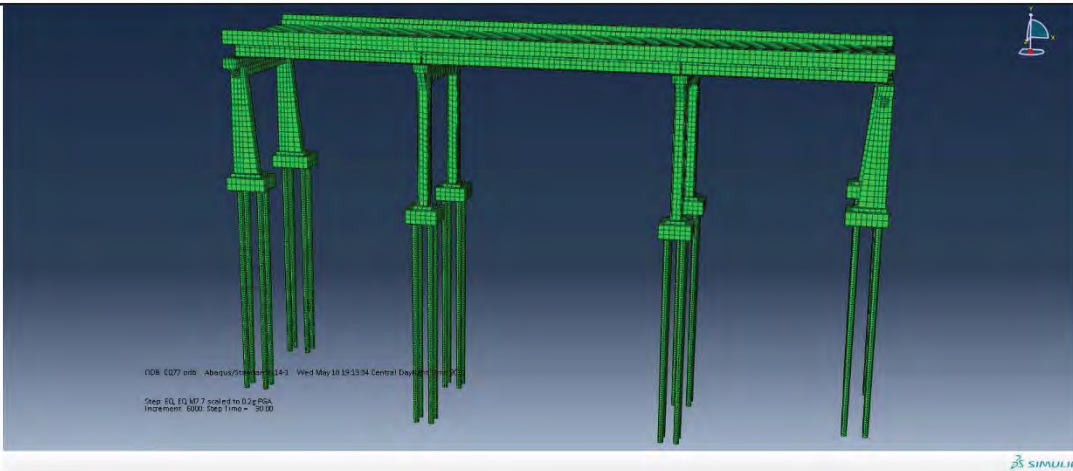
Figure 13 shows a partial side view of the model geometry or Part definition used in developing the mesh (Fig. 12). The soil is seen to have been subdivided into two layers for purposes of analysis. The top layer consists of embankment fill and roadway subgrade material added or disturbed during construction of the bridge foundation elements. The bottom layer is the naturally deposited geologic material that existed prior to bridge construction.

Boundary conditions have been applied to all side and bottom surfaces of the soil Parts preventing translation across the surface. The soil has been extended at least the length of the central span in each horizontal direction to minimize the influence of the BC on the soil stiffness and frequency.

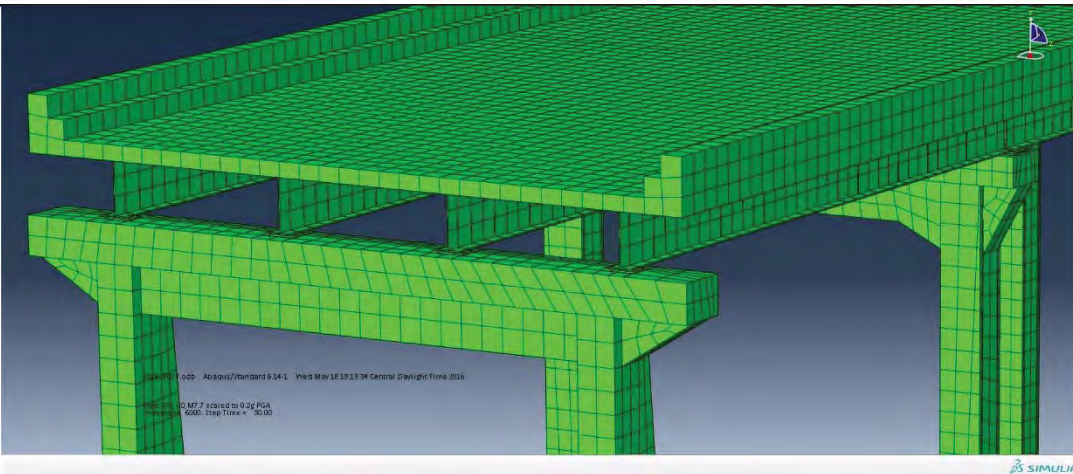




Soil-Foundation-Structure System



Structural System



Superstructure

Figure 12. Flexible system reference model mesh

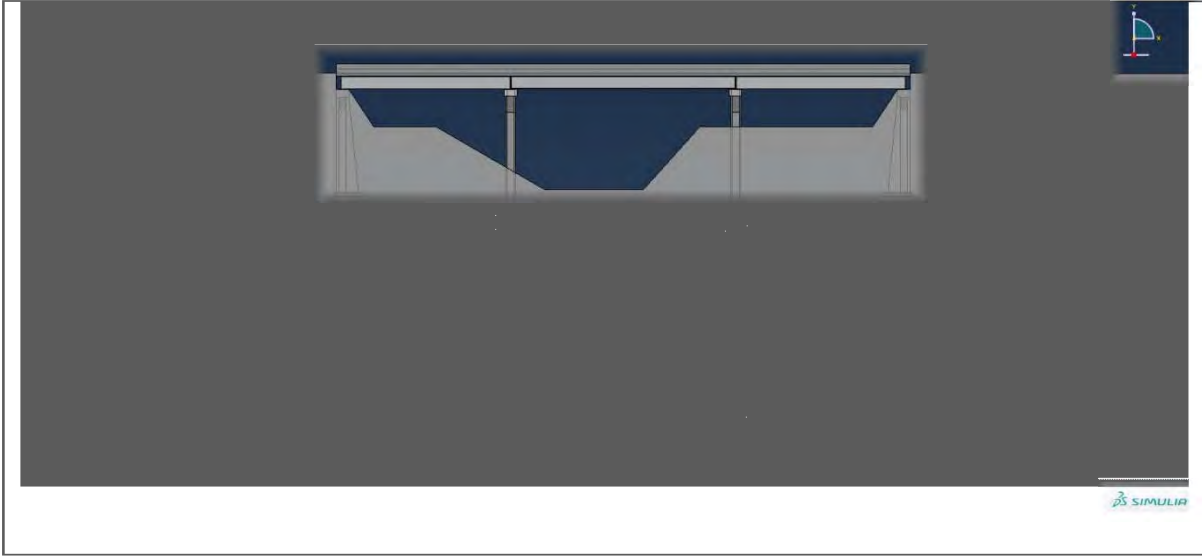
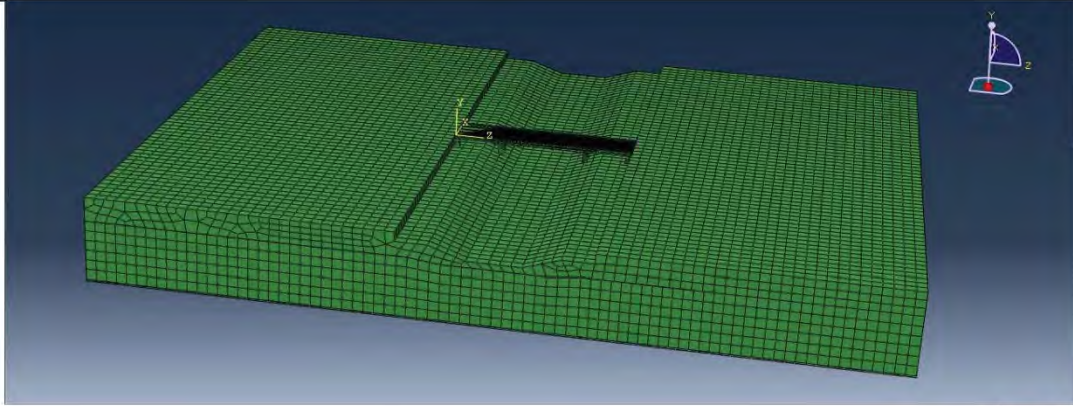


Figure 13. Flexible system part definition

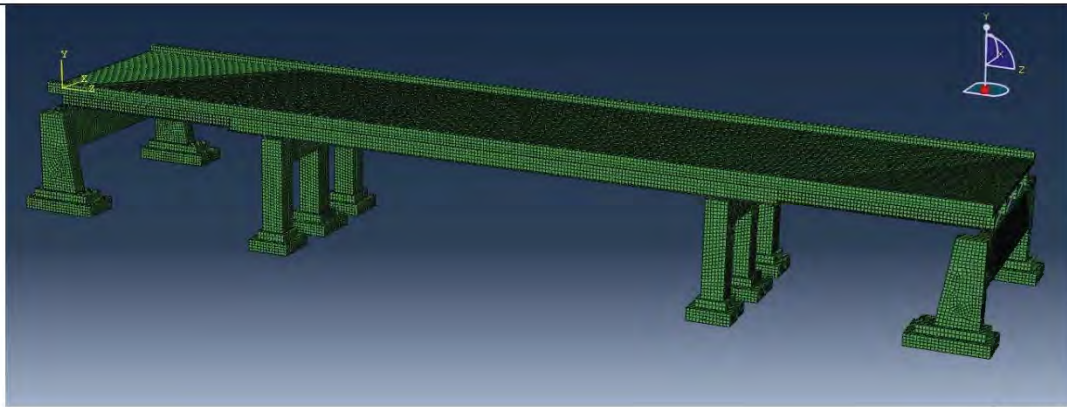
The second case (Fig. 4) consists of two 30 ft. spans and a 60 ft. center span. The superstructure is similar to the first case except that steel hot-rolled, L-shaped elements used to provide cross-bracing between girder webs. The substructure abutments are each comprised of two columns and a cap beam, whereas the piers are each comprised of three columns and a cap beam. The columns of the abutments are tapered, fully embedded in embankment soil supported on RC footings and are assumed here to sit on a thick chalk layer underlays the entire bridge foundation system. The columns of the piers are straight, partially embedded in soil, with RC footings supported on the chalk layer.

Figure 14 shows the fully meshed model geometry at subsystem and system levels. A graduate research assistant, Amir Irhayyim, documented his initial modeling of this case as the base of a masters project (8). In his project report, he provides a step-by-step description of the key features of the CAE software used to develop the component Parts and global system Assembly.

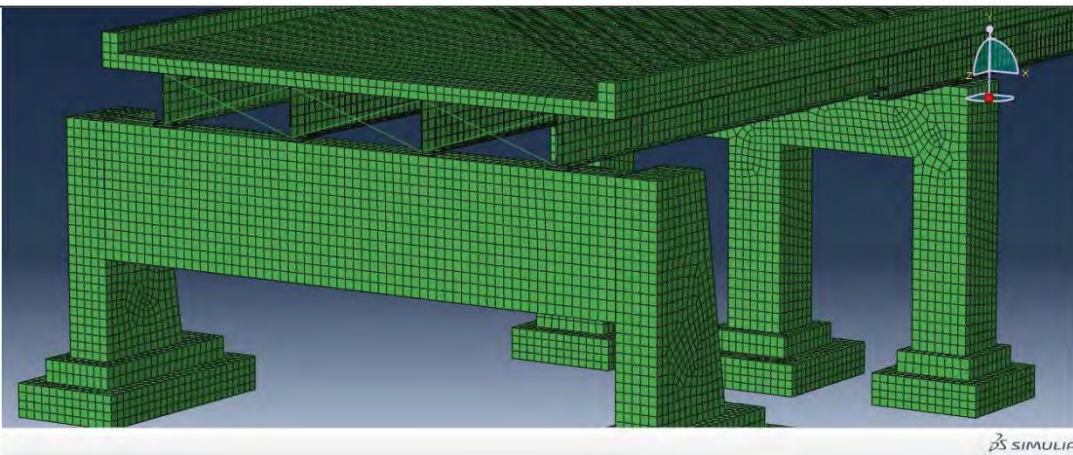
Solid elements have again been used throughout with the exception of the cross-bracing elements, where 3D beam (wire, BEAM) structural elements were considered sufficiently accurate for representing the dynamic characteristics. The point-wise cross-brace ends were connected to the girder web surfaces using a CONNECTOR interaction.



Soil-Foundation-Structure System



Structural System



Superstructure

Figure 14. Stiff system reference model mesh



Table 1 summarizes the material property data used in the concrete, steel, soil, and chalk regions of the models. These represent the project team's best interpretation of the information in data provided on drawings, soil reports, and in the literature.

Table 1. Material properties

Material	Youngs Modulus ksi	Poisson's Ratio	Weight Density lb./ft. <sup>3</sup>
Concrete	3600	.20	150
Steel	29000	.30	487
Wood (Pile)	1500	.15	40
Soil-Case 1, Top	1450	.3	115
Soil-Case 1, Bot	24656	.25	125
Soil-Case 2, Top	30	.30	125
Chalk-Case 2, Bot	300	.30	125

## Damage Scenarios

Damage here is considered either material degradation or scour around the footings. Each of these cases would in principle impact the stiffness and mass distribution. Localized damage scenarios are investigated to observe to what degree the damage induces frequency changes that are in principle measurable and to observe the degree to which the 3D nature of the modal response causes observable changes at the deck level for at least some of the characteristic lower frequency structural modes such as deck translation, longitudinal and transverse, rotation, and torsion.

Material degradation scenarios have been defined in terms of softening behavior applied to the flexible case model. The softening is localized to key components in one of two central piers and is accommodated by a reduction of the Young's modulus:

- a) Bearing plates (complete loss) beneath two girders on same side
- b) Both columns (reductions in increments of 20 percent)

A symmetric scour scenario around the footings of one pier as depicted in Figure 15.

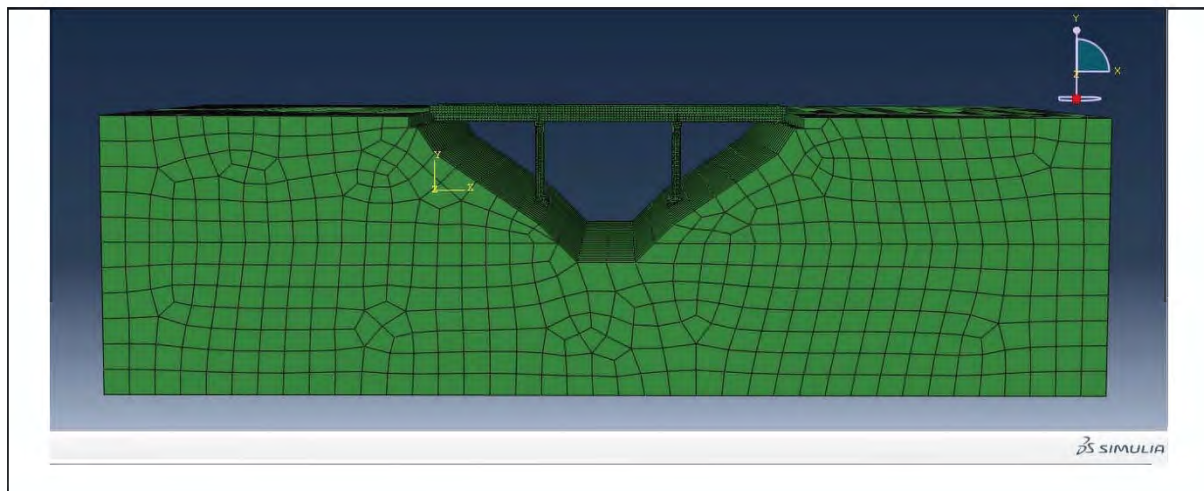


Figure 15. Flexible system symmetric scour model mesh

## DISCUSSION OF RESULTS

### Laboratory Shake Table Experiments

#### Frequency Comparisons

Figure 16 provides the frequency content of Model 1: each peak represents a natural frequency of the system without soil. The color of the peak shows dominance in the x, y, and z-directions. In Figure 6b, the shake table frequency of 20 Hz and its harmonics (40 Hz, 60 Hz, etc.) are also dominant.

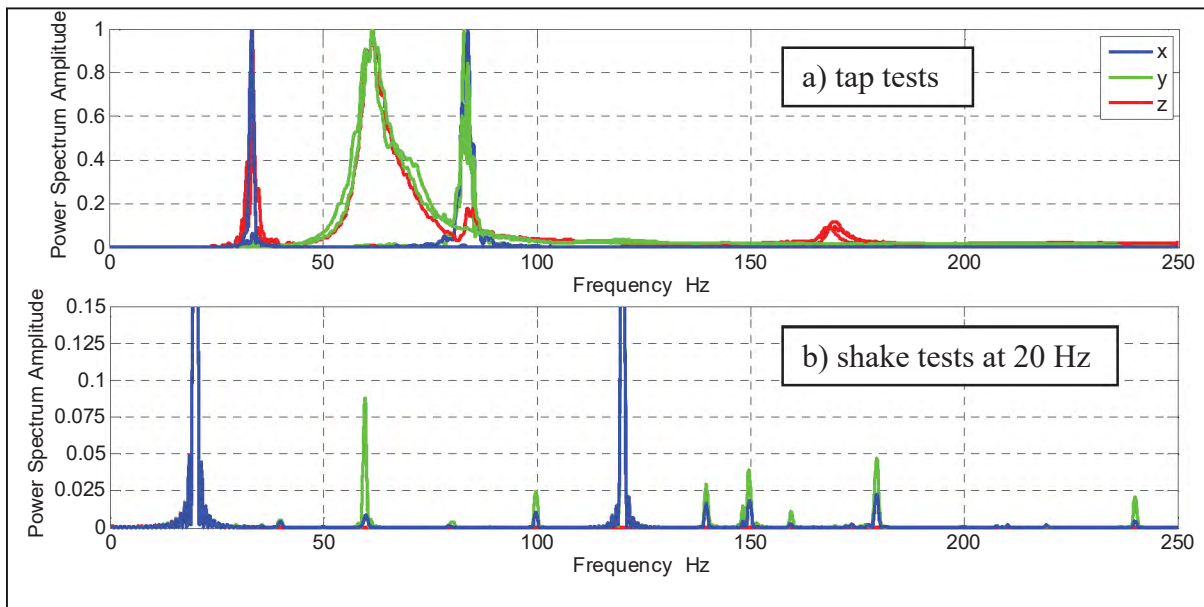


Figure 16. Power spectra for Model 1 without soil

\* Note that *x* represents sidesway, *y* longitudinal motion, and *z* vertical motion

Although identification of peaks can prove challenging, best fit results are presented in Table 2. Five modes were detected by coordinating frequencies with influential directions. The upper examined frequency was 250 Hz, and the lower was near 0 Hz or DC.

The fundamental Mode 1 occurred between 35 and 38 Hz. This mode is highly coupled, and Configuration 3 modes had more z-dominant or vertical motion. This means that the cap is more likely to displace vertically when the piles are battered. As expected, increasing the number of piles increased stiffness and thus natural frequency. In all models, this mode increased in frequency when the sand or field soil were added; the added stiffness had greater

effect than the added mass. Configuration 2 had additional modes, denoted Mode 2, that were similar x, y, and z-direction coupling due to symmetry in the straight pile configuration.

The coordinated Mode 3 is again coupled mode, but its influence varies among tested configurations. In fact, the peak was not detected for two cases. For three cases, the dominant frequencies near 50 Hz are paired with higher frequency peaks from 55 Hz to 61 Hz. For example, Model 1 has dominant longitudinal y-direction motion but is coupled with vertical motion at 49.85 Hz and with sideways at 61.5 Hz.

The coordinated Modes 4 and 5 are dominated by vertical motion. Mode 4 is strictly bending and twisting with respect to the z-direction; however, Mode 5 introduces some x and y coupling. In general, sand support caused more directional coupling than clay support.

Table 2. Natural frequencies (Hz) resulting from tap and shake tests.

Coordinated Mode #		1	2	3		4	5	
Model 1	No Sand	33.35	-	49.85 (YZ)	61.5 (XY)	190.1	208.9	217.0 224.0
	Sand	34.71	-	-		-	-	
	Clay	35.55	-	49.50	56.1 (XZ) 61.0 (YZ)	189.0	208.7	
Model 2	No Sand	35.05	40.3	-		-	212.0 (XZ)	
	Sand	36.10	40.5	51.10	55.5 (Z)	192.0	-	
	Clay	38.95	44.5	57.05		-	222.5 (X)	
Model 3	No Sand	38.10	-	55.50		197.5	210.5 (XZ)	224.5 (YZ)
	Sand	38.20	-	59.50		196.0	220.5	

Tables 3 and 4 present the results of finite element modeling Models 1 and 3 without soil. The ABAQUS models were built using estimated boundary conditions and material properties: thus, these numerical simulations are not expected to match, but trend comparisons can be drawn. Note also that finite element mode results are rarely as coupled as experimental results.

Table 3 shows the first four modes of ABAQUS Model 1, the railroad bridge. The structure is fixed at all surfaces, which in turn generates Modes 1 and 2. Table 4 reveals that the y translation mode only occurs: the friction fit at the cap of Model 3 has released the bending moment capability. Otherwise, adding four additional batter piles increased the natural frequency by 16%.

The addition of the four battered piles and the moment release cap connections make the structure more susceptible to torsion. The frequency at which vertical bending and twisting occur decreases by 39%.

Lastly, the massive cap begins to bend at 425 Hz and 675 Hz for Models 1 and 3, respectively. The flexing direction switches between the two cases. Upon deep examination, higher frequencies are local column modes.

Table 3. Natural frequencies and mode shapes resulting from finite element Model 1


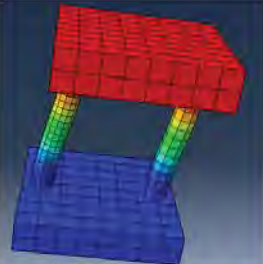
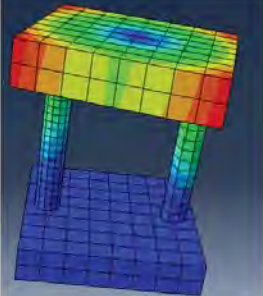
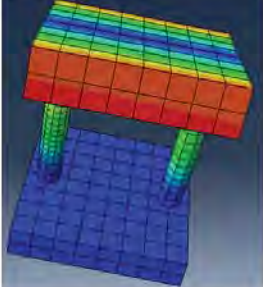
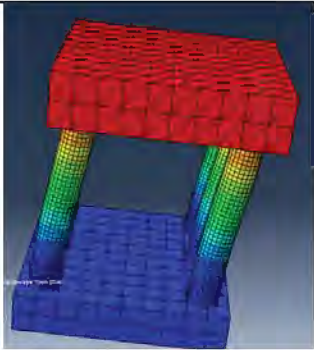
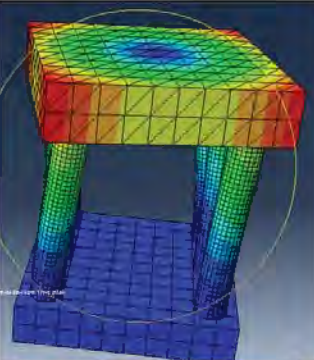
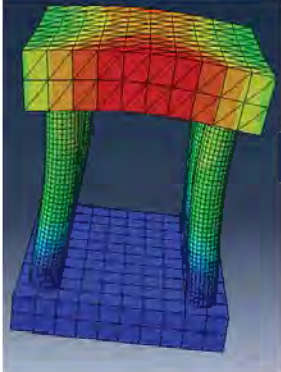
Mode	Frequency (Hz)	Description	Mode Shape
1	74.76	Pure translation in the y-direction	
2	106.28	Translation in the +y-direction; bending of columns in the y-direction	
3	202.82	Bending in the z-direction; twisting about the z-direction	
4	425.68	Cap flex along centerline	

Table 4. Natural frequencies and mode shapes resulting from finite element Model 3

Mode	Frequency (Hz)	Description	Mode Shape
1	86.72	Pure translation in the y-direction	
-	-	Translation with bending not found	
3	123.37	Bending in the z-direction; twisting about the z-direction	
5	674.74	Cap flex along centerline	

Comparisons between experimental and modeled results are provided in Table 5. Rather than direct contrast, the ratio between frequencies of Model 3 to Model 1 is presented as a better comparison. The dominant y-translation effects increase by the nearly same percentage within 1.58%. Only Model 1 showed the beam bending in the ideal realm of finite element modeling. The dominant vertical z-direction effects do not agree because of the aforementioned moment release connections. The cap flexing was mainly vertical for the



finite element models but highly coupled in the experimental modes; the frequencies are significantly different, even by ratio, for cap flexing modes.

Table 5. Comparison of experimental to modeled natural frequencies

Experimental Results			FE Modeling Results			General Description of Mode
Model 1	Model 3	Ratio of Model 3 to 1	Model 1	Model 3	Ratio of Model 3 to 1	
33.35	38.10	1.142	74.76	86.72	1.160	Pure translation in the y-direction; coupled XYZ for experimental data
-	-	-	106.3	-	-	Translation in the +y-direction; bending of columns in the y-direction
190.1	197.5	1.039	202.8	123.4	0.608	Z-direction effects; bending and twisting.
208.9	210.5	1.007	425.7	674.7	1.585	Cap flex along centerline; coupled XYZ for experimental data. Additional modes located nearby.
217.0	-					
224.0	224.5					

## Temporal Comparisons

Time history comparisons were performed through both accelerations and deflections. The maximum response magnitudes are used as a metric for comparison.

Table 6 presents the steady state peak acceleration for configurations without soil and with field soil. While the shake table's frequency remained constant at 20 Hz, the levels of acceleration were approximately double and then tripled. During testing, a hysteretic check was performed by reducing the table's 0.21 g back down to 0.10 g: the difference in readings was minimal at an average of 1.56%. This ensures that premature damage was not induced, except for the aforementioned Model 3 with field soil.

The raw readings do not have much significance, except to show that all three directions were simultaneously excited in the system. In general, the x-direction provided the maximum response as expected since that is the excitation direction. To make a direct comparison, an amplification factor is defined as the system's output response divided (or normalized) by the table's input. This ratio varies from 2.56 to 4.30, meaning that the table's acceleration is magnified in the structures by 256% to 430%.

In Model 1, the field soil serves to increase the acceleration that the system experiences. However, the 0.34 g level shows a significant difference from all other measurements. The vertical z-direction acceleration is the absolute greatest of any configuration while the excited



x-direction is the minimum of any case. Therefore, a premature column failure at the base is suspected, and this reading should be discarded.

The ultimate result is that all configurations experience more acceleration when field soil is added. The amount of increased response varies from 11% to 130%, and this trend does not appear to have a linear or monotonic effect with increasing excitation.

Table 6. Maximum tri-axial accelerometer results for tested configurations

Configuration	Table Accel. (g)	Maximum Acceleration at Steady State (g)			Amplification Factor	
		X Sway	Y Long.	Z Vert.	X Sway	W/Field Soil Added
1 No Soil	0.1	0.3406	0.0491	0.0499	3.41	-
1 Field Soil	0.1	0.3918	0.0256	0.0705	3.92	+0.51
2 No Soil	0.1	0.3001	0.0623	0.0493	3.00	-
2 Field Soil	0.1	0.4302	0.1880	0.1446	4.30	+1.30
3 No Soil	0.1	0.3052	0.0575	0.0523	3.05	-
3 Field Soil	-	N/A	N/A	N/A	-	-
1 No Soil	0.21	0.6703	0.0742	0.098	3.19	-
1 Field Soil	0.21	0.8737	0.0466	0.1839	4.16	+0.97
2 No Soil	0.21	0.5645	0.0562	0.0509	2.69	-
2 Field Soil	0.21	0.5877	0.0778	0.0608	2.80	+0.11
3 No Soil	0.21	0.5861	0.0691	0.0584	2.79	-
3 Field Soil	-	N/A	N/A	N/A	-	-
1 No Soil	0.34	1.0364	0.1131	0.1447	3.05	-
1 Field Soil	0.34	0.2881	0.1502	0.3505	0.85	-2.20*
2 No Soil	0.34	0.8520	0.0589	0.0557	2.51	-
2 Field Soil	0.34	0.8895	0.0877	0.0696	2.62	+0.11
3 No Soil	0.34	0.8706	0.0853	0.1330	2.56	-
3 Field Soil	-	N/A	N/A	N/A	-	-

\*Premature failure

The deflections obtained by high speed video analysis have also been compared via steady-state magnitudes. Deflections are more likely to provide a smooth result as they cycle at one-quarter of the rate of acceleration. The detailed analysis of the captured video's tracked data is provided in Appendix A and is summarized herein.

The high speed video analysis reliably reached an accuracy of thousandths of an inch. Comparisons at 0.1 g table acceleration were still difficult to quantify. The front view of the

structure provides the resultant of only x and z direction measurements, and thus it does not necessarily reflect the three-dimensional coupled rotation, translation, and torsion.

Generally, increasing table amplitude increases the structure's response as expected. However, the increases are not proportional to the table's acceleration. Responses with field soil appear less predictable than with sand, but only two field soil cases could be tested.

In comparing configurations at 0.1 g, displacement appears to increase from Model 1 to Models 2 and 3, but these measurements are quite small. At 0.21 g, Point 1 increases in motion from Model 1 to 2 to 3, but Point 2 does the exact inverse. At 0.34 g, the largest deflections occur at Point 1 of Model 3 and Point 2 of Model 1.

The soil supporting conditions significantly affect the deflections of the video analysis. The sand cases move less at low table accelerations: field soil cases move 82.3% to 300.5% more. At higher table accelerations, the contrary occurs: the field soil cases move less by 48.1% to 98.0%. This trend is true for all three models.

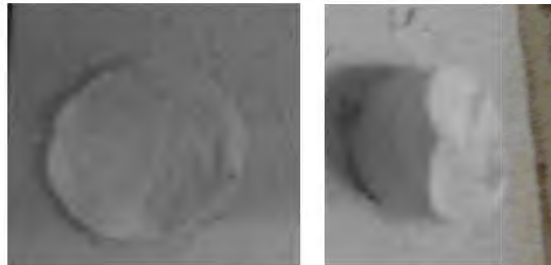
The final step was to shake Models 1 and 2 until failure. Frequency analysis led to a structural sensitivity at 35 Hz, and thus shaking commenced there and proceeded with increasing amplitude.

Figure 17 shows the tipping failure of Model 1 and the footing fractures. Note that right column failed first, and then the left column suddenly fractured flat: this selected the direction of tipping.

Figure 18 shows Model 2's failure. Note that Point 1 was visibly lifting up and slamming down while the "8" column was vibrating laterally. Upon removal of the cap, five of six columns were broken, yet the structure did not collapse. The footing fractures in Figure 8b show two cases: both columns sheared off near the base, but the left column was displaced off of its base. Note how the damp field soil held its shape, providing redundant support preventing significant cap displacement. It is remarkable that so many failures existed yet global stability was maintained.



a. Video still



b. Footing fractures

Figure 17. Failure of Model 1



a. Video still



b. Footing fractures

Figure 18. Failure of Model 2

## Finite Element Modeling

### Reference Case Modal Characteristics

Static self-weight analysis was first performed to develop initial stress and deformation conditions and to evaluate overall integrity of the assembled reference models shown in Figures 12 and 14, respectively. Eigenvalue analysis was then performed to obtain the mode shapes and frequencies of the assembly.

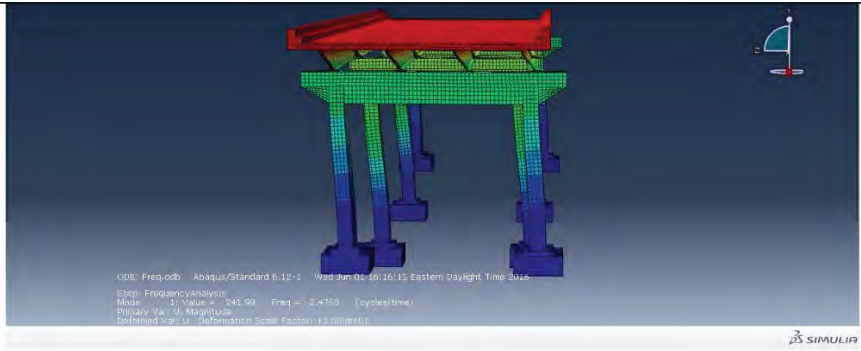
Preliminary analysis was performed in stages as a check on the model performance. First, the superstructure was fixed at the bearing level to obtain the characteristic behavior of the composite deck system. Next, the substructure was added and the base of the footings restrained to define a fixed base model to obtain the characteristic behavior of the structural system. Last, the soil and piles were added to obtain the characteristic SSI system.

Addition of the soil and piles in the SSI system introduces numerous additional modes. This makes it difficult to identify characteristic modes associated with the resistance to the structural system provided by the soil system and structure. Here the fixed base frequencies and mode shapes are used to define the characteristic structural system modes, and a search of a limited number of modes in the neighborhood of the fixed base modal frequencies is then performed. Sequential display of the mode shapes for this subset of modes is then used to confirm the SSI mode corresponding to the comparable fixed base one.

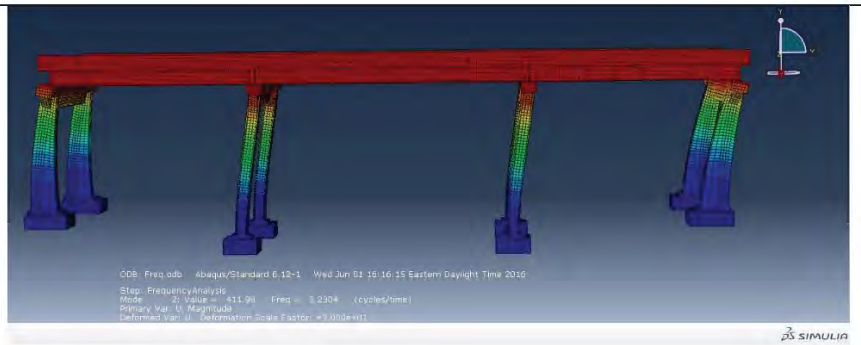
Modal characteristics of the first three modes for each system are summarized in Table 7. Figures 19 and 20 show characteristic modes for the fixed base models of the flexible and stiff systems, respectively.

Table 7. Modal characteristics of fixed base reference models for two case studies

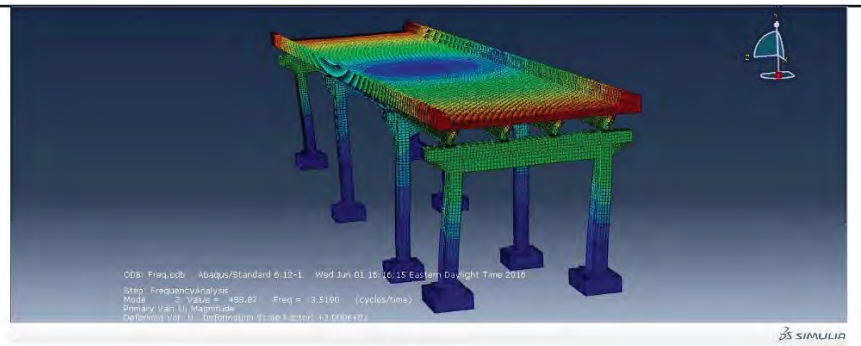
Mode Number	Flexible System		Stiff System	
	Frequency, Hz	Deck Movement	Frequency, Hz	Deck Movement
1	2.48	Transverse	7.06	Vertical
2	3.23	Longitudinal	7.25	Out-of-Plane Rotation
3	3.52	In-Plane Rotation	8.78	Longitudinal



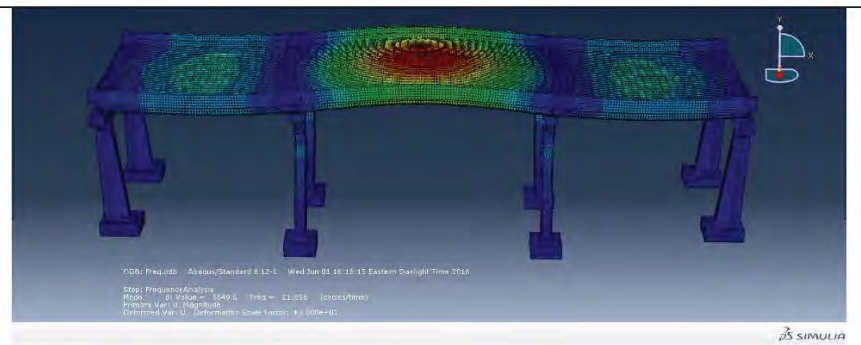
Transverse Mode 2.48 Hz



Longitudinal Mode 3.23 Hz

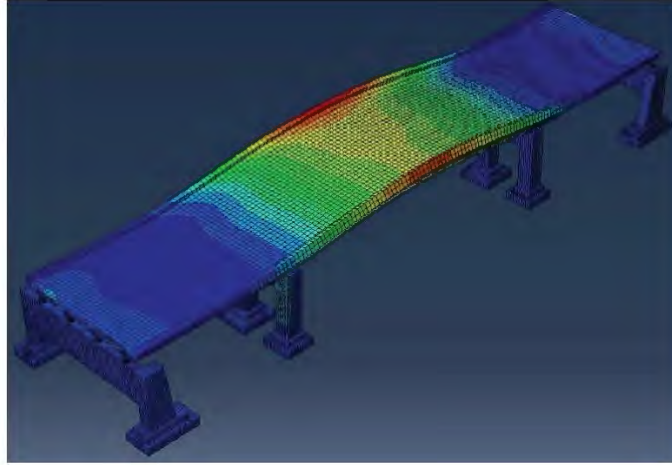


Rotation Mode 3.52 Hz

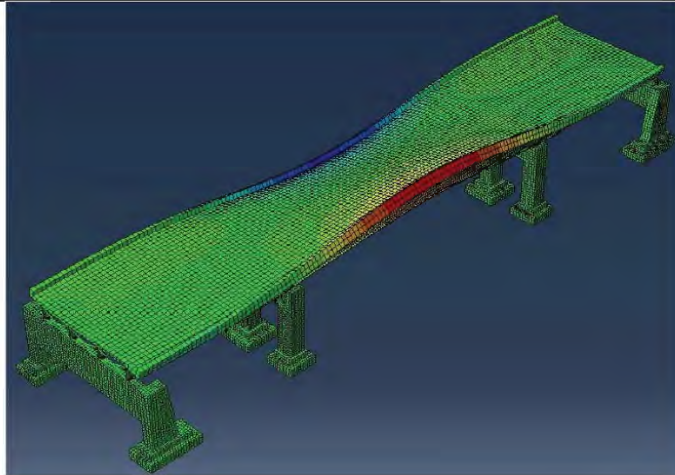


Vertical Mode 11.9 Hz

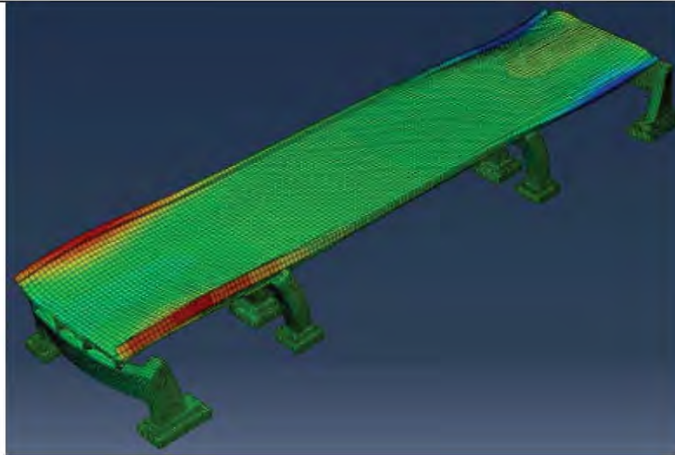
Figure 19. Fixed base modes for the flexible system



Vertical Mode 7.06 Hz



Center Span Deck Torsion Mode 7.25 Hz



Longitudinal Mode 8.78 Hz

Figure 20. Fixed base modes for the stiff system



The top three modes shown in Figure 19 are the lowest three modes for the fixed base model of the flexible system. The fundamental mode is lateral translation at a relatively low frequency of about 2.5 Hz. This mode involves movement of the deck and substructure mass laterally. Without the cross-bracing this movement causes severe bending in double-curvature of both the girder webs and the columns below. The deck slab remains flat as it translates essentially as a rigid body. In the second mode, at about 3.2 Hz, the deck slab and girders translate longitudinally as a rigid body inducing out-of-plane bending of the piers and abutments. In the third mode, at about 3.5 Hz, the deck slab rotates as a rigid body inducing anti-symmetric in-plane bending of the columns. Vertical translation of the center span deck slab is exhibited in the eighth mode at about 11.9 Hz. The fourth through seventh modes involve counterbalancing translation of pier and abutment pairings.

The top three modes shown in Figure 20 are the lowest three modes for the fixed base model of the stiff system. The fundamental frequency of about 7.1 Hz, and the fundamental mode is now vertical translation of the center span deck. The second mode, at about 7.2 Hz, is rotation of the center span deck about the centerline or the roadway which induces torsional deformation in the deck slab. The third mode, at about 8.7 Hz, is longitudinal translation of the deck inducing out-of-plane bending of the columns. Without any soil to resist the translation, the abutment cap beam bends significantly.

Comparing the flexible and stiff systems, it is first noted that the fundamental fixed base frequency of the stiff system is nearly three times higher than than of the flexible system. This is mostly due to the difference in column size and number. The relative order of the characteristic modes in terms of frequency is also quite different. This is primarily due to differences in center and side span lengths. The aspect ratio of center/side span length for the flexible system is roughly 4:3 whereas that for the stiff system is closer to 2:1.

The SSI models include the foundations supporting the fixed base systems which introduce changes to the modal characteristics. The nature of the changes are often complex and subject to many issues including choice of material properties, boundary conditions, and interactions at contact surfaces. Here these effects are demonstrated through the SSI model of the flexible system which will than be the focus of the study of the additional effects of damage.

Table 8 compares the frequencies computed for the characteristic modes for the fixed base and SSI reference models for the flexible system.

Table 8. Modal characteristics of reference models of flexible system

Deck Movement	Fixed Base	SSI
	Frequency, Hz	Frequency, Hz
Longitudinal	3.23	2.03
Transverse	2.47	2.06
In-Plane Rotation	3.52	2.12
Vertical	10.0	10.0

Figure 21 shows how each of the characteristic mode shapes identified in Figure 19 involving horizontal deck movement is altered by incorporating SSI. The soil has been removed for clarity. Figure 22 shows the characteristic mode involving vertical deck movement. The soil has been included here and illustrates the faceted appearance of the relatively coarse soil mesh when amplified 30 times to highlight the bending action in the stiffer structural elements.



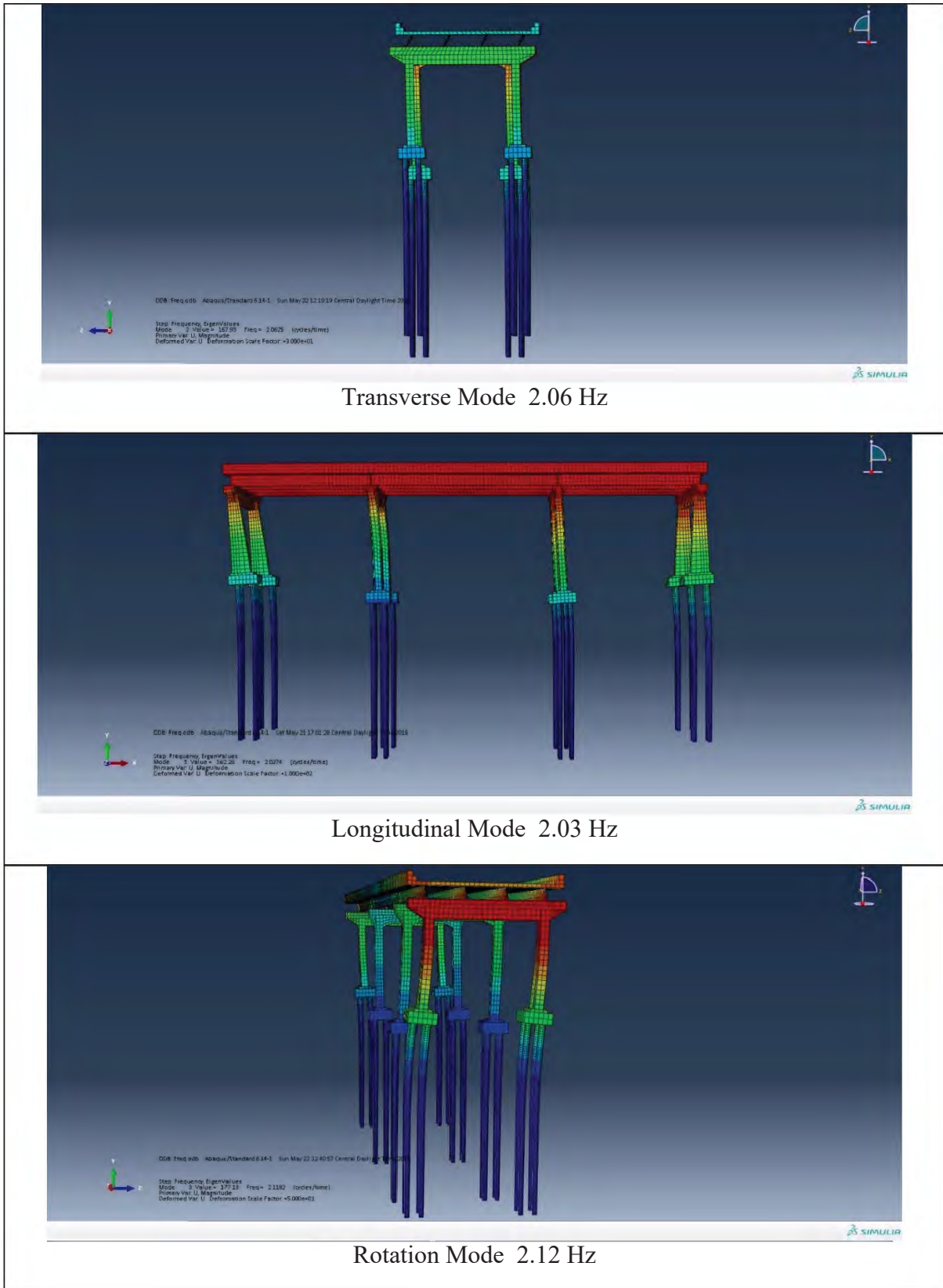


Figure 21. SSI modes for the flexible system involving horizontal deck movement

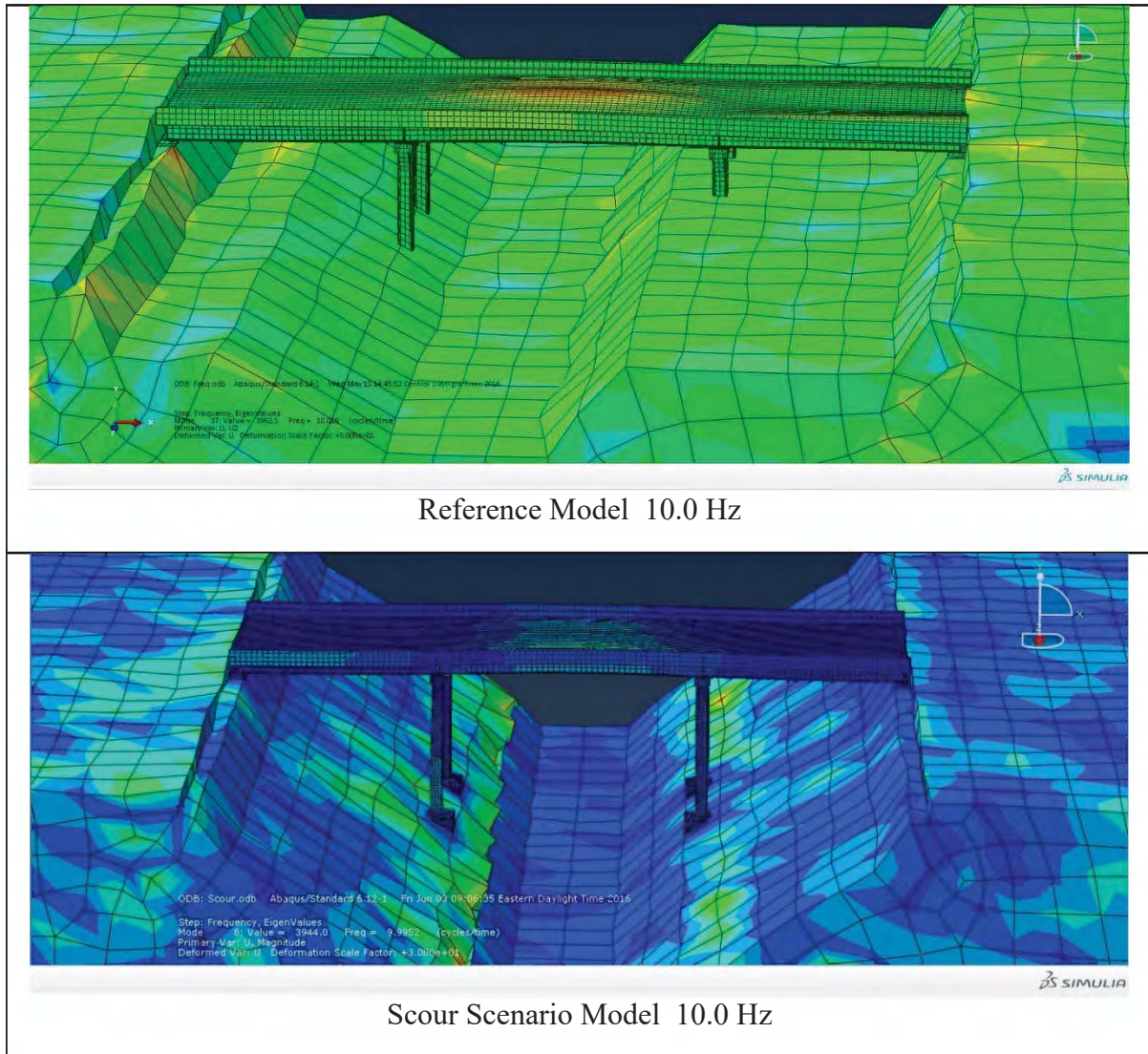


Figure 22. SSI mode for the flexible system involving vertical deck movement

## Damage Scenario Modal Comparisons

Frequencies for characteristic modes of the material deterioration damage scenario models of the SSI flexible system were not noticeably different from those of the reference model. It is possible other modes than the four characteristic ones were influenced more noticeably, but it is not clear whether such modes would be detectable at the deck level.

No noticeable difference was found in the vertical mode of the symmetric scour damage scenario model of the SSI flexible system (see Fig. 22). Significant changes of about 20 percent, however, were observed in the computed modes involving horizontal deck motion. Table 9 compares the frequencies computed for the reference and symmetric scour scenario models of the SSI flexible system.

Table 9. Modal characteristics comparison of SSI models for flexible system

Deck Movement	As Constructed	Symmetric Scour	
	Frequency, Hz	Frequency, Hz	% Reduction
Longitudinal	2.03	1.54	24
Transverse	2.06	1.69	18
In-Plane Rotation	2.12	1.66	22



## CONCLUSIONS

The ability to detect damage in substructures of highway and railway bridges using modal vibration techniques performed at the superstructure deck level is investigated as a means to improve nondestructive testing evaluation in cases where visual inspection is difficult or impossible.

Detailed finite element analysis is performed to characterize the modal characteristics of two aging operational three-span highway bridges accessible to the project team. The bridges have similar superstructures but are distinguished by their substructures and the geologic formations on which they are founded. One has a deep foundation or flexible system, and the other a shallow or stiff one.

Fixed base models of the reference or as-constructed conditions indicate that the first three frequencies for the two structural systems involve horizontal movement of the superstructure deck and are significantly different in both order and magnitude of their frequencies.

Soil-structure interaction models incorporating the soil and foundation elements indicate that these features induce significant softening of these characteristic modes relative to the fixed base ones.

Damage scenarios involving material deterioration of substructure elements of one of the central piers of the flexible system do not appear to induce any noticeable changes in the modal characteristics of the soil-structures interaction models. For a symmetric scour scenario considered, however, modes involving horizontal movement of the deck mass exhibit a significant reduction in frequency that would be detectable at deck level.

Tests on lab scale models of substructure subsystems in three configurations of increasing relative stiffness and stability are conducted on a shake table. Frequencies obtained from accelerometer measurements provide insight to variations in frequency and temporal dynamic response characteristics for the different configurations. Similar insight under idealized boundary conditions are obtained by simplified finite element analysis of the subsystems.

Modal characteristics and dynamic response patterns observed by processing of the measurements indicate modal coupling not detectable from the idealized finite element models. Furthermore, the measurements indicate that the influence of cohesionless and cohesive soils on the dynamic characteristics may depend on frequency, moisture, and contact surface conditions.

## RECOMMENDATIONS

Many factors contribute to the dynamic characteristics of relevance to the detection of damage impacting the structural integrity and stability of aging bridges. The focus of the FE analysis performed in this study is on dynamic response characteristics of the soil-foundation-structure system whose properties are often difficult to assess or observe through visual inspection.

A detailed solid modeling approach has been adopted to account for many of the complex 3D aspects of geometry and component interactions of importance to the detection of damage. Even though many simplifications have been made in order to make the problem tractable, generation and post-processing of the analysis models required significant learning curves even for the graduate research assistants involved in the project. The same may be said for the construction of lab scale models, execution of shake table testing, and data acquisition and processing.

Sustaining such a complex modeling and testing knowledge base throughout the three year duration of the study during which multiple students often contributed for only short durations proved challenging. For successful expansion of the understanding of the complex effects of damage, it is recommended that continued training and project funding opportunities be made available by the transportation industry to sustain technical personnel in academia, research, and practice.

The findings of the study demonstrate that scour may detectably soften dynamic characteristics of bridge soil-foundation-structure systems whereas material deterioration is more problematic and may require another approach to detect reliably.

The study also demonstrates that the soil and foundation elements noticeably soften the fixed base modal characteristics even in the absence of damage. Their influence should be accounted for in any comparisons of computational model and measurement based response.

In light of the study's findings, it is recommended that further attention, through both computational and measurement based studies, be given to obtaining a better understanding of the nature and extent of the various softening tendencies for a variety of aging bridge cases found throughout the national inventory. With a better understanding of these tendencies, field measurements may then be interpreted more reliably, and detection may become more sensitive to varying levels and types of damage.



## ACRONYMS, ABBREVIATIONS, AND SYMBOLS

%	percent
DOF	degree-of-freedom
FE	finite element
FHWA	Federal Highway Administration
ft.	foot (feet)
g	acceleration due to gravity
Hz	Hertz or cycles per second
ksi	kilopounds per square inch
lb.	pound(s) force
MDOT	Mississippi Department of Transportation
MS	Mississippi
NBI	National Bridge Inventory
NCITEC	National Center for Intermodal Transportation and Economic Development
NDT	Non-destructive Testing
NI	National Instruments
RC	reinforced concrete
SSI	soil-structure interaction
UM	University of Mississippi
US	United States





## REFERENCES

1. National Bridge Inventory, February 2016. FHWA, U.S. Department of Transportation. <http://www.fhwa.dot.gov/bridge/nbi.cfm> . Accessed May 27, 2016.
2. Ervin, E., Aranchuk, V., Mullen, C., and Chambers, J. “Three Integrated Projects to Enhance Non-Contact Rail Inspection Technology for Application to Substructure Health Evaluation on Both Rail and Road Bridges.” Final Report to NCITEC, Project No. UM 2013-24, University of Mississippi, January 2014.
3. Ryan, T.W. et al. Bridge Inspector’s Reference Manual (BIRM). Publication No. FHWA NHI 12-049, FHWA, U.S. Department of Transportation, National Highway Institute, December, 2012.
4. Swann, C. and Mullen, C. “Predicting Erosion Impact on Highway and Railway ridge Substructures.” Final Report to NCITEC, Project No. UM 2013-26, University of Mississippi, May 2016.
5. Multi-Function Dynamics Laboratory. University of Mississippi. <http://www.engineering.olemiss.edu/~eke/MFDL/index2.html>. Accessed May 27, 2016.
6. ABAQUS/CAE User’s Guide, Version 6.14, Simulia, Dassault Systemes, 2014, <http://abaqus.software.polimi.it/v6.14/index.html> . Accessed May 29, 2016.
7. ABAQUS Analysis User’s Guide, Version 6.14, Simulia, Dassault Systemes, 2014, <http://abaqus.software.polimi.it/v6.14/index.html> . Accessed May 29, 2016.
8. Irhayyim, A. “Creating a Model of a Bridge with ABAQUS/CAE.” Project report submitted in partial fulfillment for the degree of Master of Science in Engineering Science, University of Mississippi, November, 2015.